Environ Monit Assess (2021) 193: 429
https://doi.org/10.1007/s10661-021-09192-x

Forecasting shoreline changes along the Egyptian Nile Delta coast using Landsat image series and Geographic Information System

Khalid Dewidar · Sahar Bayoumi

Received: 8 September 2020 / Accepted: 1 June 2021 / Published online: 19 June 2021

Abstract Before construction of the Aswan High Dam, the Nile Delta was expanding and advancing into the Mediterranean Sea. Subsequently, it became a highly destructive Delta due to the lack of sediment discharge, climate change, subsidence, and coastal processes (e.g. wind, waves, tides, and littoral currents). Many coastal structures have been erected to stop or mitigate coastal problems in the study area. We used 31 Landsat images to monitor the fluctuation of erosion and deposition along the study area. The shorelines in these huge datasets were extracted using standard techniques. Linear regression ratio (LRR) and end-point rate (EPR) were used with Digital Shoreline Analysis System (DSAS) software to determine the rates of beach changes; we then forecast future shoreline changes. The accuracy of the model's results was checked using the ground field measurements of several studies. This model also creates an estimate of the position uncertainty at each time step. The value of the uncertainty is low (approximately half a pixel) along the shorelines without coastal protection. This study aimed to forecast future beach evolution to the year 2041 to evaluate its sensibility and facilitate proposals for coastal protection for human safety and habitats if the coastal processes and climate change continue to worsen with time.

Keywords Forecast · Shoreline change · Nile Delta · DSAS program · Landsat series · GIS

K. Dewidar (✉)
Geography Department, College of Arabic Language & Social Studies, KSA, Qassim University, Riyadh, Saudi Arabia
e-mail: k.dewidar@qu.edu.sa

K. Dewidar
Environmental Science Department, Faculty of Science, Damietta University, New Damietta City, Egypt

S. Bayoumi
IT Department, College of Computer and Information Science, King Saud University, Riyadh, Saudi Arabia

S. Bayoumi
IT Department, Institute of Graduate Studies & Research, Alexandria University, Alexandria, Egypt

Introduction

The Mediterranean Delta coast is essential to the Egyptian people, who depend on it for food, residential areas, recreation, and internal and external communication. The Nile Delta is densely populated (200–400 people/km^2) and hosts a full range of industrial, agricultural, and tourism activities (Mostafa et al., 2014). The Mediterranean Delta coast extends more than 280 km from west of Rosetta to Port Said city (Fig. 1). This coastline is very dynamic, altered by erosion and sedimentation processes, especially at its prominent headlands. The main cause of beach changes on the Egyptian Delta beach is the suspension of sediment supply from the Nile River due to the construction of barrages and dams along the river.

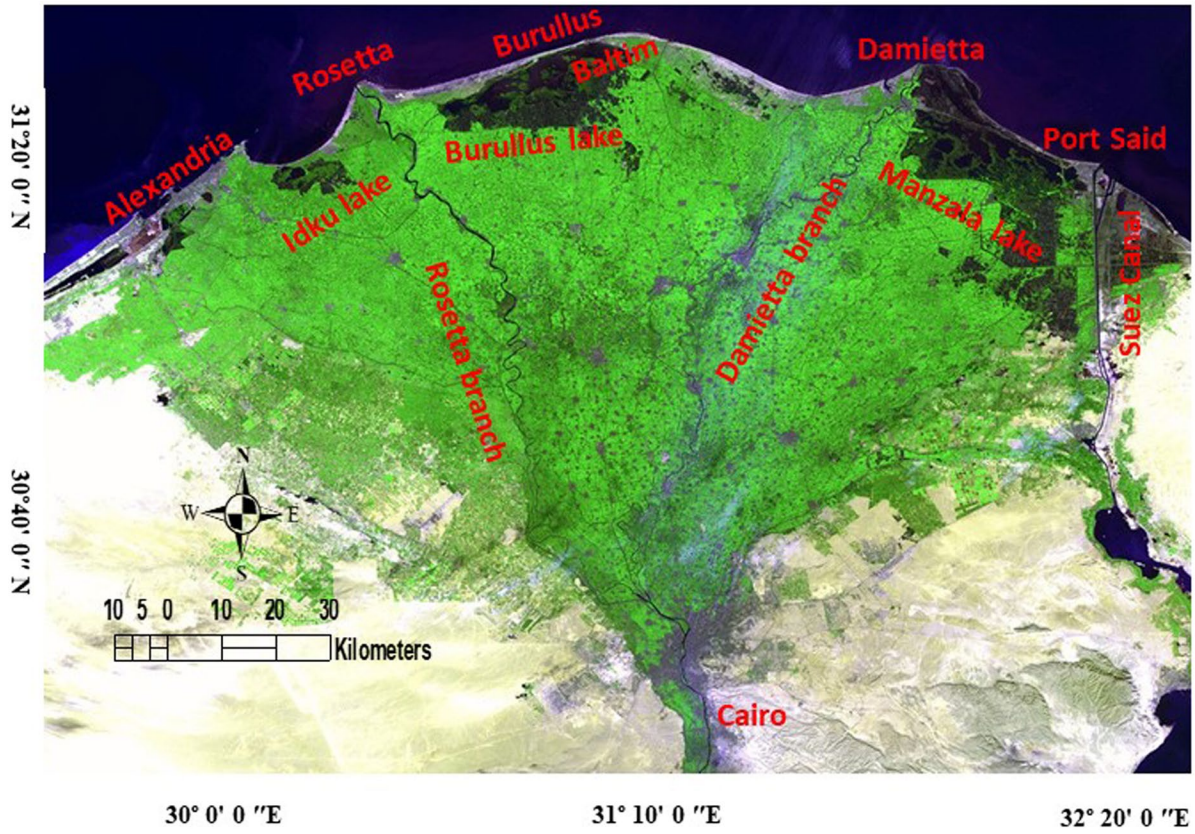

Fig. 1 Geographic location of the Nile Delta coast

This is compounded by the natural reduction of Nile floods due to climate change and coastal processes. Several protection works have been established to minimize coastal changes along the coast of the study area, including seawalls, groins, dikes, jetties, and breakwaters. The Shore Protection Agency has invested $10,000,000/year in protection measures over the last 10 years (CORI, 2010). These coastal works have completely stopped further erosion of the Rosetta and Damietta headlands and have caused beach changes along other parts of the Egyptian Mediterranean coast. Therefore, there is a need for further investigations and periodic monitoring, due to the persistence of these beach changes, to identify the factors and causes of the coastal problem, to enable forecasting future beach changes, and to prepare a comprehensive sustainable strategy for managing coastal areas.

Several previous studies have found changes in the pattern of erosion and sedimentation on the coast of the Nile Delta. Many studies (Dewidar & Frihy, 2007; Frihy & Komar, 1993; Frihy, 2010, 2010b; Sestini, 1989; Stanley, 1988) have determined that erosion rates in the Rosetta headland are the highest along the delta coast (−96 m/year). These eroded sediments are transported by coastal currents to the west to Abu Qir Bay and east to Abu Khashaba, where they are deposited along both sides of the Rosetta branch, which leads to beach accretion at a maximum rate of 16.8 m/year. Erosion along the Burullus–Baltim headland has been replaced by accretion (13.26 m/year). The main reason for this evolution is the reinstallation of a series of shore-parallel breakwaters and vertical groins. Originally, this area experienced an erosion rate of approximately −5 m/year. These previous studies also show that the rate of erosion was about –43 m/year in the Damietta headland before the establishment of a 6-km seawall in 2000. In addition, the severe erosion beside the Ras El Bar resort was restored by a

few deposition shapes (15 m/year) resulting from the creation of eight detached breakwaters parallel to the beach line.

Many researchers have used the Digital Shoreline Analysis System (DSAS) to detect shoreline changes at various places in the world. Natesan et al. (2013) used DSAS for a shoreline change analysis of the Vedaranyam coast, India. Pérez-Alberti et al. (2013) used it to map shoreline changes along the coast of Galicia, Spain. Temitope and Oyedotun (2014) indicated that DSAS was a useful tool for calculating rates of change in southwest England from multiple historical shoreline positions and sources. Murat et al. (2019) used DSAS to assess changes before and after construction of dams in the Yesilirmak basin and shoreline changes in the delta in northern Turkey. Mullick et al. (2020) used DSAS to detect the positional change of the Ganges deltaic coast of Bangladesh. Also, in Egypt, other researchers have used DSAS to detect shoreline changes between different dates of satellite data (Darwish et al., 2017; Ghoneim et al., 2015). Based on these selected studies, DSAS is considered an accurate and reliable tool for detecting shoreline changes.

The objectives of this study included further monitoring of the Egyptian Nile Delta for 46 years and updating its coastal geomorphology to determine appropriate protection measures in the long term. In addition, this is the first study, to our knowledge, to use DSAS to forecast the future coastal location for the year 2041. The huge volume of time-series satellite data available can detect small shoreline changes. This approach will help decision-makers put forward a future plan to protect the Egyptian Nile Delta coast, if coastal processes and climate change continue to worsen with time.

Study area

The Nile Delta coast extends from 30° 0′E to 32° 20′E and from 30° 40′N to 31° 20′N (Fig. 1), with a total area of about 17,848 km^3. The study area is a triangle with its apex at Cairo city and its base along the Mediterranean Sea. It includes six major cites—Alexandria and Rosetta to the west, Burullus and Baltim in the middle, and Damietta and Port Said to the east. The area includes five local governorates—from the west Alexandria, El Beheira, and Kafr El Shiekh, and Damietta and Port Said to the east. About 19 million people live in the coastal Nile Delta area. In addition, 40% of Egyptian agricultural products come from the Nile Delta. The climate is Mediterranean—hot in summer and moderate in winter. The maximum temperature is 40 °C in August, and the minimum is 10 °C in winter months.

Physical settings of the Nile Delta

Geomorphologically, the Nile Delta consists of beaches, coastal dunes, deserts, and lakes. The beaches are covered by loose sand ranging in mean grain size from 0.11 to 0.40 mm (very fine to medium sand) (Frihy & Komar, 1993). Frihy and Komar (1993) investigated the pattern of beach changes and correlated them with longshore distribution ratios of heavy minerals and sediment grain size. They also examined the eroded areas and found a high rate of beach erosion associated with finer grain and heavy minerals. The Nile Delta coastal dunes consist of longitudinal and crescent shapes originating from the former Sebennitic branch approximately 6500 years ago (Stanley & Warne, 1993). These dunes are located near Idku, El Burullus, Baltim, and Gamasa. Most of these coastal dunes were damaged and removed during construction of the Ras El Bar resort and vacation services (El Banna & Frihy, 2009). Three coastal lakes are located on the Egyptian Nile Delta coast. These lakes (Idku, Burullus, and Manzala Lakes) receive a large amount of agricultural drainage, sewage, and industrial liquid waste before being discharged into the Mediterranean Sea. A study by Fanos et al. (1995) found that the prevailing wind direction on the coast of the Egyptian Nile Delta during the year (50–60%) is from the north and northwest direction, while the northeastern winds account for 10–15%. The average wind speed is seasonal in intensity, at 3–5 m/s in summer and spring and 5–7 m/s in winter, with a higher rate from the NW (El Banna & Frihy, 2009). The Delta coast is typically wave- and current-dominated (Coleman et al., 1981; Manohar, 1981). Wave action along the Egyptian Delta coast is seasonal in nature, responding to changing wind systems over the water where the waves are generated (Gad et al., 2013). Frihy et al. (2010a, 2010b) produced wave rose diagrams for different areas along the Nile Delta coast. The tide waves along the

Egyptian Mediterranean coast are semi-diurnal, with a range of less than 30 cm. Iskander et al. (2007) measured wave records along the Nile Delta coasts from 1985 to 2010 and recorded an increasing trend in sea wave height from 2.6 to 2.9 cm/year.

Protection structures along the Nile Delta

Several coastal protection structures, including jetties, groins, seawalls, and breakwaters, were built along the promontories of the Egyptian Nile Delta to combat beach changes and reduce inlet siltation. To control erosion at the Rosetta headland, two 5-km-long seawalls composed of artificial embankments covered by 4–7-ton concrete blocks of angled shape were installed between 1988 and 1991 to the west and east of the mouth of the Rosetta branch (Frihy & Lotfy, 1994). The seawalls stand 6.75 m above the mean sea level and their widths vary from 45 to 70 m (Fig. 2A). Additional coastal structures were built to control erosion at both the eastern and western ends of the seawalls (Frihy et al., 2010a, 2010b). These included five groins constructed in 2003 with lengths ranging between 400 and 500 m seaward, spaced 800–900 m apart. Then, in 2005, construction began on another ten short groins (80–150 m long) at distances of 500 to 600 m on the lee side of the western seawall (Frihy et al., 2010a, 2010b). Farther east, a concrete 600-m-long jetty was built in 1950 to protect the eroding beach downstream of the Burullus inlet. To the east of this jetty, a basalt riprap approximately 1.3 km in length was constructed. More recently, a new fishing harbour has been built at the western limit of this sector immediately adjacent to the Burullus inlet (Fig. 2B). The inner harbour basin is protected by two jetties, one of which is from the previously built entrance jetty. Recently, the Burullus–Baltim area was protected by a series of parallel detached breakwaters and nine short groins (Fig. 2C) (Frihy et al., 2010a, 2010b). These series include 14 detached breakwaters that were installed between 1993 and 2004. In addition, two detached breakwaters were built approximately 3 km east of the Burullus inlet. Each breakwater extends 250–350 m parallel to the beach. The breakwaters are 220 m from the shore and spaced 320–400 m apart. These breakwaters were constructed at a depth between 3 and 4 m in the active surf zone (Frihy et al., 2010a, 2010b). These protection works helped stop erosion and build sedimentation forms in this area. Also, they worked to stop the movement of beach sediments towards the

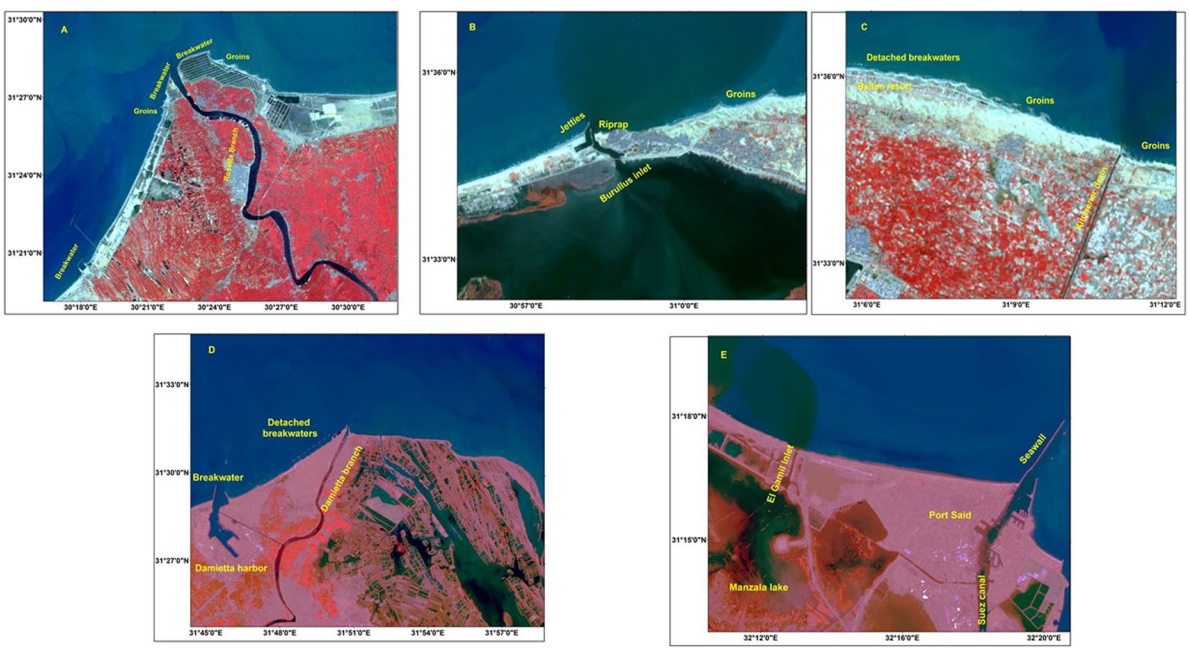

Fig. 2 Coastal protection structures along the Nile Delta coast

east, leading to accelerated erosion at the eastern end of the breakwater system. This erosion has been mitigated by the construction of nine short groins. At the Damietta promontory, two jetties were constructed to protect the entrance of the Damietta inlet from silting between 1941 and 1963 (Dewidar & Frihy, 2010, 2010b). Eight detached breakwaters were built between 1991 and 2002 to stop erosion along the Ras El Bar Resort (Fig. 2D) (Frihy & Dewidar, 2003). Farther west, two breakwaters were constructed in 1992 on both sides of Damietta Harbour to prevent deposition in the shipping channel (Frihy et al., 2003). Two large seawalls are constructed along the entrance of Suez canal to prevent siltation processes (Fig. 2E).

Materials and methods

The beach shoreline of the Egyptian Nile Delta coast was extracted from the Landsat satellite series over 46 years (1972–2018) (Table 1). Landsat satellite data allow the creation of the current location of coastlines at a relatively low cost. Also, developed image processing software, such as Erdas Imagine, v. 15, helps improve the accuracy of feature extraction. The Landsat image series were downloaded from the US Geological Survey EROS Center. The supplied images were geometrically and radiometrically corrected. The first images were rectified to the most recent 2018 Landsat images for the east (path 38/176) and west (path 38/177) Nile Delta. AutoSync software in Erdas Imagine was used for all Landsat image data. Image rectification accuracy was < 0.5 pixels. To extract the shoreline position, the image threshold was set using Band 4 (0.8–1.1 µm) for MSS, Band 7 (2.0–2.35 µm) for TM/ETM^{+}, and Band 7 (2.11–2.29 µm) for OLI. The dataset was converted to form a binary image or image mask (a value of zero for water and one for land). In order to ensure waterline mapping accuracy in the case of MSS image data, 3 × 3 edge enhancement filters were used to sharpen the boundary between water and land classes. Binary images (masked images) were used as input layers in the unsupervised classification module to form complete separation between land class and water class and to remove the effect of suspended materials due to longshore sediment transport. Horizontal and vertical

Table 1 The acquisition date, Landsat number, Landsat sensor, pass/row, and spatial resolution in meters used in the study area

The acquisition date of West Delta	The acquisition date of East Delta	Satellite number	Landsat sensor	Path/Row	Spatial resolution (m)
31–08-1972	31–08-1972	Landsat-1	MSS	190/38	57
03–01-1973	03–01-1973	Landsat-1	MSS	189/38	57
————	20–09-1984	Landsat-5	TM	176/38	28.5
10–08-1990	04–08-1990	Landsat-5	TM	177/38–176/38	28.5
17–06-1993	11–04-1995	Landsat-5	TM	177/38–176/38	28.5
18–04-1997	07–06-1998	Landsat-5	TM	177/38–176/38	28.5
10–11-2000	11–11-2000	Landsat-7	ETM +	177/38–176/38	28.5
17–06-2002	24–08-2003	Landsat-7	ETM +	177/38–176/38	28.5
09–08-2004	18–06-2005	Landsat-7	ETM +	177/38–176/38	28.5
12–06-2006	04–03-2007	Landsat-7	ETM +	177/38–176/38	28.5
————	18–01-2008	Landsat-7	ETM +	176/38	28.5
————	05–02-2009	Landsat-7	ETM +	176/38	28.5
07–02-2010	31–05-2010	Landsat-7	ETM +	177/38–176/38	28.5
————	30–12-2012	Landsat-7	ETM +	176/38	28.5
————	20–03-2013	Landsat-7	ETM +	176/38	28.5
06–03-2014	11–02-2014	Landsat-8	OLI	177/38–176/38	28.5
11–03-2016	04–03-2016	Landsat-8	OLI	177/38–176/38	28.5
26–02-2017	03–02-2017	Landsat-8	OLI	177/38–176/38	28.5
14–12-2018	22–02-2018	Landsat-8	OLI	177/38–176/38	28.5

Source of data: https://earthexplorer.usgs.gov/

Sobel filters were used for each unsupervised classified image on each date to enhance edge detection. Some editing to remove small objects and fill holes is formed for each filtered image on each date. The filtered images for each date were converted to vector layers using the raster-to-vector module (Dewidar & Frihy, 2007; Frihy, 2010, 2010b). All extracted shoreline vectors are used as shape files in ArcGIS, version 10.8. DSAS program, version 4.4, is used as an extension of ArcGIS software.

The DSAS program (Thieler et al., 2017) was used to generate 2330 sections with 100 m horizontal distance and perpendicular to the coast. These transects were then plotted over the shorelines extracted from remote sensing data to establish the rates of shoreline changes along the Egyptian Nile Delta coast (Fig. 3A). Endpoint rate (EPR) and linear regression rate (LRR) were used to compute the rate of beach changes. The EPR was calculated by dividing the distance of the horizontal shoreline movement by the time elapsed between the oldest and most recent measurements (Ali & Narayana, 2015; Crowell et al., 1997). LRR was determined by fitting the least-square regression line to all comparable shore points for different durations for a given segment (Dolan et al., 1991; Suhura et al., 2018). Positive EPR and LRR values represent shoreline movements toward the sea (i.e. the rate of accretion), and negative values indicate movements away from the sea (i.e. the rate of erosion). These values were plotted along the shoreline for a length of approximately 233 km from the west Nile Delta to the east Nile Delta (Fig. 3B).

LRR values were used to model shoreline changes along the Nile Delta coast (Kalman, 1960) (Fig. 4A). This model begins in 1972 (the earliest date) and forecasts the shoreline position for each successive time step until another shoreline observation becomes available. The model minimizes the error between the modelled and observed shoreline positions to improve the forecast, including updating the rate and uncertainties (Barman et al., 2014; Long & Plant, 2012). Then, the updated rate of shoreline change is used to forecast successive time steps until another survey date is reached, and new data are processed again in the model. This model is ideal for the Nile Delta for many reasons (Fig. 4B). First, all shoreline data were extracted from a single source (Landsat image series). Second, the pattern of erosion and sedimentation along the coast of the Egyptian Nile Delta follows a linear regression analysis, as mentioned by Dewidar and Frihy (2010, 2010b). Third, the coastal processes have had the same magnitude for a long time. Fourth, the pattern of erosion and sedimentation along the coast of the Egyptian Nile Delta is known by most researchers (Darwish et al., 2017; Frihy et al., 2010a, 2010b).

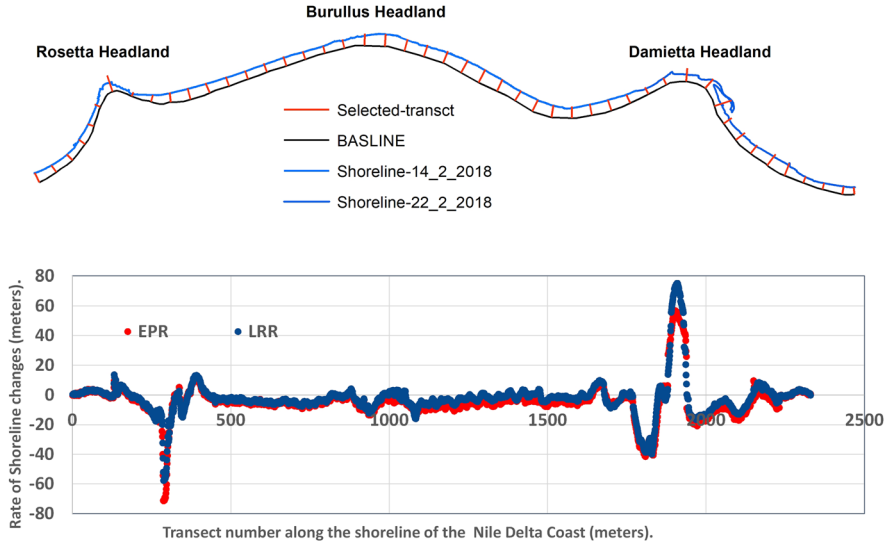

Fig. 3 Transects plotted over the shorelines extracted from remote sensing data **A**, and long-term shoreline changes in the Nile Delta (the linear regression rate (LRR) and the end-point rate (EPR) were calculated using the DSAS program **B**

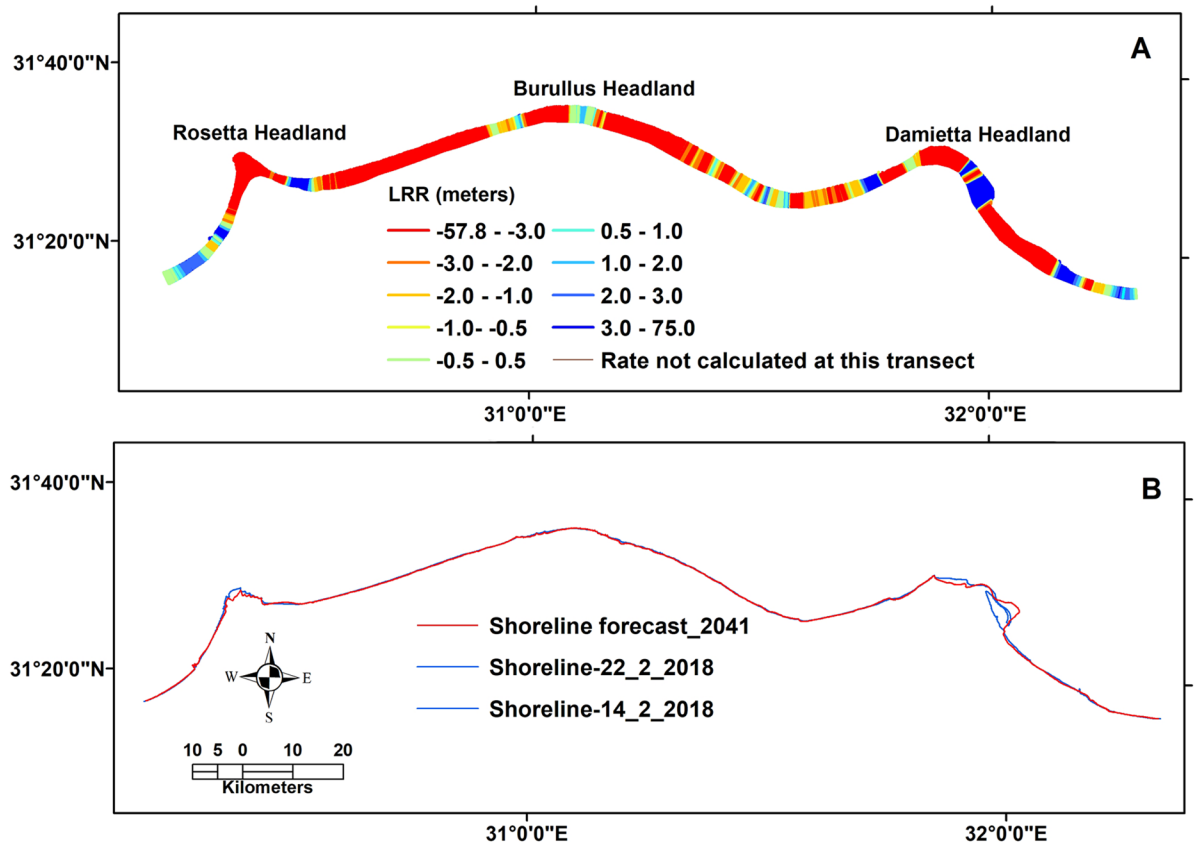

Fig. 4 LRR values resulted from the model **A**, and shoreline of the year 2041 forecasted using a Kalman filter versus the shoreline of dated 2018 along the Nile Delta **B**

Results and discussion

The shoreline database was used to calculate long-term shoreline changes. The rates of beach retreat were determined by comparing the beach positions over 46 years. Approximately 2330 transects were made across the shore baseline (Fig. 3A). EPR and LRR were used to calculate the rate of beach changes along the Egyptian Nile Delta (Fig. 3B). To evaluate the accuracy of the results, beach change rates were compared with field measurements obtained by Dewidar and Frihy (2010, 2010b, 2007) and Frihy and Komar (1993), as well as the findings of Darwish et al. (2017). Also, the results of Ghoneim et al. (2015) are completely consistent with the results of this research, especially in the Rosetta promontory section. The patterns of erosion and accretion match well, although our study depends on huge Landsat time-series datasets and future prediction shoreline modelling for the year 2041.

The three headland regions along the Egyptian Nile Delta coast have suffered erosion and sedimentation. The Rosetta headland initially showed a high rate of erosion at more than – 54.1 m/year (Figs. 4A and 5A). This value is identical to that found by Frihy et al. (2010a, 2010b). Sediments are being deposited in the Idku sink at a rate of 6 m/year. On the other side of the Rosetta headland, Abu Khashba forms a significant region of the sink, where the rate of deposited sediments is 11.46 m/year (Fig. 5A). The El Burullus headland has suffered erosion at a rate between –20 and –3 m/year (Fig. 5B). Various coastal protection structures have been established in this area to reduce erosion. Some protection works have been installed inside the Burullus inlet, including two breakwaters to protect the inlet of the fishing harbour. Likewise, on its eastern side, there are seawall and riprap protection structures (Fig. 2B).

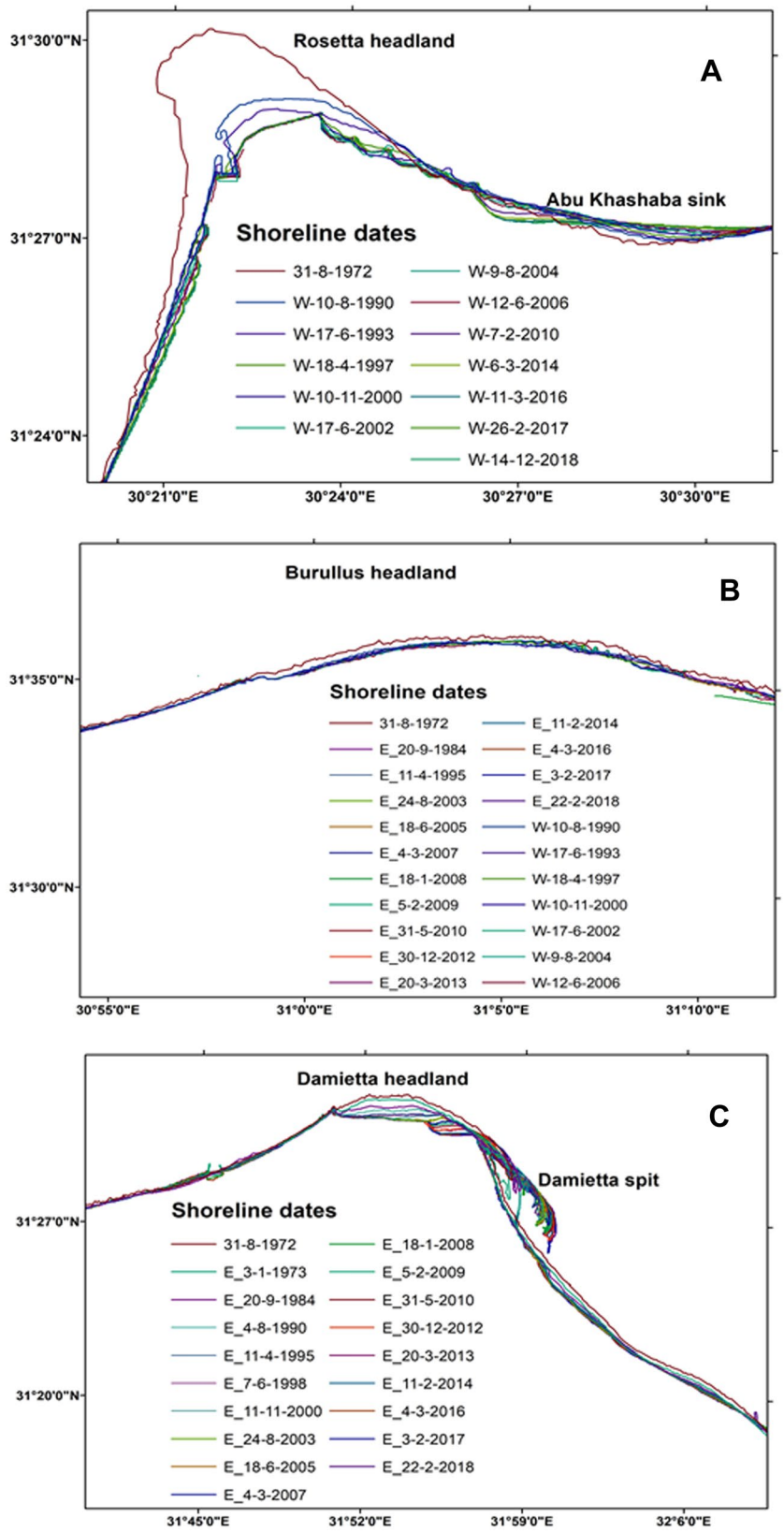

Fig. 5 Shoreline changes along the Nile Delta coast, Rosetta headland **A**, Burullus headland **B**, and Damietta headland **C**

At the Baltim Resort, there are 14 detached breakwaters to protect swimmers and tourism investments. The Gamasa sink receives all the eroded sediments from the Burullus headland, and, based on the calculations of this study, the rate of sedimentation in this region ranges from 2 to 3 m/year (Figs. 4A and 5B). Moving to the east, we find the Damietta headland. A long seawall was constructed parallel to the beach of Damietta headland to stop the erosion process (Fig. 2D). The eroded sediments from the Damietta headland drift into two parts—the Ras El Bar Resort to the east and the Damietta Spit to the west. Nine detached breakwaters were built along the coast of the Ras El Bar resort to protect swimmers and the infrastructure. Now, this resort suffers a rip current caused by installing vertical groins along the beach. Also, suspended sediments pass through the Damietta harbour causing siltation. This result was revealed by El-Asmar and White (2002). Therefore, additional soil dredging is necessary to maintain the appropriate harbour depth for ships. Based on this research, the rate of erosion at the western side of the Damietta promontory ranges from -0.5 to -2 m/year (Figs. 4A and 5C). Also, on the eastern side of the Damietta promontory, the accretion rate ranges from 60 to 75 m/year, forming the Damietta Spit. This deposition is continually reshaped based on the direction of wave action and the dominant littoral current. Farther toward the Port Said breakwater, there is additional deposition of sediment eroded from the Damietta headland. These processes cause siltation and sedimentation along the Manzala lake and El Gamil inlets (Fig. 2E). Application of this model in the study area affirmed, with a high degree of confidence, the behaviour of beach erosion and accumulation, if the conditions of natural coastal processes and protection work are not changed. The predicted shoreline positions for the year 2041 and shoreline positions of image dated 2018 were superimposed in Fig. 4B. In this study, forecasting long-term rates of erosion and sedimentation indicated that they will remain at the same rates unless additional protection structures interrupt the overall pattern (Fig. 4B). In addition, this model showed disruptions in the pattern of erosion and sedimentation due to the installation of new groins, especially in the eastern part of the Rosetta Branch.

Conclusions

Erosion and sedimentation rates were calculated over 46 years for a 233-km stretch along the study area. The three headlands of the Nile, the shape of the Delta coast, suffer from erosion and accretion. The rate of beach changes depends on the beach profile equilibrium, wave action, and the littoral current. A forecast model for studying erosion and sedimentation rates has demonstrated that coastal structures built to stop or reduce erosion are effective. In the long term, climate change will cause catastrophic situations in low-lying areas around the world, particularly along the Egyptian Nile Delta coast. Consequently, it is essential to conduct more investigations and monitoring of coastal areas, especially the Mediterranean coast of Egypt. The application of this model succeeded in clarifying general patterns of erosion and sedimentation along the coast of the Egyptian Nile Delta, which should encourage decision-makers to develop strategic plans and protection measures.

Acknowledgements The authors thank the Deanship of Scientific Research and RSSU at King Saud University for their technical support.

Funding This research project was supported by a grant from the "Research Center of the Female Scientific and Medical Colleges", Deanship of Scientific Research, King Saud University.

References

Ali, P. Y., & Narayana, A. C. (2015). Short-term morphological and shoreline changes at Trinkat Island, Andaman and Nicobar, India, After the 2004 Tsunami. *Marine Geodesy, 38*(1), 26–39. https://doi.org/10.1080/01490419.2014.908795

Barman, N., Chatterjee, S., & Khan, A. (2014). Trends of shoreline position: An approach to future prediction for Balasore Shoreline, Odisha, India. *Open Journal of Marine Science, 5*, 13–25. https://doi.org/10.4236/ojms.2015.51002

Coleman, J. M., Roberts, H. H., Murray, S. P., & Salama, M. (1981). Morphology and dynamic sedimentology of the eastern Nile delta shelf. *Marine Geology, 42*(1), 301–326. https://doi.org/10.1016/0025-3227(81)90168-7

CORI. (2010). *Proposal for EGYPT, Review: Literature and Arts of the Americas*.

Crowell, M., Douglas, B. C., & Leatherman, S. P. (1997). On forecasting future U.S. shoreline positions: A test of algorithms. *Journal of Coastal Research*, *13*(4), 1245–1255. JSTOR.

Darwish, K., Smith, S. E., Torab, M., Monsef, H., & Hussein, O. (2017). Geomorphological changes along the Nile Delta

coastline between 1945 and 2015 detected using satellite remote sensing and GIS. *Journal of Coastal Research, 33*(4), 786–794. https://doi.org/10.2112/JCOASTRES-D-16-00056.1

Dewidar, Kh., & Frihy.O. (2010). Automated techniques for quantification of beach change rates using Landsat series along the north-eastern Nile Delta, Egypt. *Journal of Oceanography and Marine Research, 1*(2), 28–39. https://www.longdom.org/archive/ocn-volume-1-issue-2-year-2010.html

Dewidar, Kh., & Frihy, O. (2007). Pre- and post-beach response to engineering hard structures using Landsat time-series at the north-western part of the Nile delta, Egypt. *Journal of Coastal Conservation, 11*(2), 133–142. https://doi.org/10.1007/s11852-008-0013-z

Dolan, R., Fenster, M. S., & Holme, S. J. (1991). Temporal analysis of shoreline recession and accretion. *Journal of Coastal Research*, *7*(3), 723–744. JSTOR.

El Banna, M. M., & Frihy, O. E. (2009). Human-induced changes in the geomorphology of the north-eastern coast of the Nile delta, Egypt. *Geomorphology, 107*(1), 72–78. https://doi.org/10.1016/j.geomorph.2007.06.025

El-Asmar, H. M., & White, K. (2002). Changes in coastal sediment transport processes due to construction of New Damietta Harbour, Nile Delta, Egypt. *Coastal Engineering, 46*(2), 127–138. https://doi.org/10.1016/S0378-3839(02)00068-6

Fanos, A. M., Khafagy, A. A., & Dean, R. G. (1995). Protective works on the Nile Delta coast. *Journal of Coastal Research*, *11*(2), 516–528. JSTOR.

Frihy, O., Deabes, E. A., Shereet, S. M., & Abdalla, F. A. (2010a). Alexandria-Nile Delta coast, Egypt: Update and future projection of relative sea-level rise. *Environmental Earth Sciences, 61*(2), 253–273. https://doi.org/10.1007/s12665-009-0340-x

Frihy, O., Deabes, E., & Sayed, W. (2003). Processes reshaping the Nile Delta promontories of Egypt: Pre- and post-protection. *Geomorphology, 53*, 263–279. https://doi.org/10.1016/S0169-555X(02)00318-5

Frihy, O. E., & Komar, P. D. (1993). Long-term shoreline changes and the concentration of heavy minerals in beach sands of the Nile Delta, Egypt. *Marine Geology, 115*(3), 253–261. https://doi.org/10.1016/0025-3227(93)90054-Y

Frihy, O. E., Deabes, E. A., & Gindy, A. A. E. (2010). Wave climate and nearshore processes on the Mediterranean coast of Egypt. *Journal of Coastal Research*, *26*(1), 103–112. JSTOR.

Frihy, O. E., & Dewidar, K. M. (2003). Patterns of erosion/sedimentation, heavy mineral concentration and grain size to interpret boundaries of littoral sub-cells of the Nile Delta, Egypt. *Marine Geology, 199*(1), 27–43. https://doi.org/10.1016/S0025-3227(03)00145-2

Frihy, O. E. & Lotfy, M. F. (1994). Mineralogy and textures of beach sands in relation to erosion and accretion along the Rosetta promontory of the Nile Delta, Egypt. *Journal of Coastal Research*, *10*(3), 588–599. JSTOR.

Gad, M. A., Saad, A., El-Fiky, A., & Khaled, M. (2013). Hydrodynamic modeling of sedimentation in the navigation channel of Damietta Harbor in Egypt. *Coastal Engineering Journal*, *55*(2), 1350007–1–1350007–1350031. https://doi.org/10.1142/S0578563413500071

Ghoneim, E., Mashaly, J., Gamble, D., Halls, J., & Abu-Bakr, M. (2015). Nile Delta exhibited a spatial reversal in the rates of shoreline retreat on the Rosetta promontory comparing pre- and post-beach protection. *Geomorphology, 228*, 1–14. https://doi.org/10.1016/j.geomorph.2014.08.021

Iskander, M. M., Frihy, O. E., El Ansary, A. E., Abd El Mooty, M. M., & Nagy, H. M. (2007). Beach impacts of shore-parallel breakwaters backing offshore submerged ridges, western Mediterranean coast of Egypt. *Journal of Environmental Management, 85*(4), 1109–1119. https://doi.org/10.1016/j.jenvman.2006.11.018

Kalman, R. E. (1960). *A new approach to linear filtering and prediction problems.* Transaction of the ASME–Journal of Basic Engineering. https://doi.org/10.1115/1.3662552

Long, J. W., & Plant, N. G. (2012). Extended Kalman Filter framework for forecasting shoreline evolution. *Geophysical Research Letters, 39*(13), 13603. https://doi.org/10.1029/2012GL052180

Manohar. M. (1981). Coastal processes at the Nile Delta coast. *Shore Beach, 49*(1), 8–15.

Mostafa, A. T. T., Sato, S., & Tajima, Y. (2014). Quantitative estimation of longshore sediment transport based on thermoluminescence: Two case studies around Tenryu and Nile River mouths. *Journal of Coastal Research, 30*(3), 537–547. https://doi.org/10.2112/JCOASTRES-D-13-00050.1

Mullick, M.R.A., Islam, K.M.A. & Tanim, A.H. Shoreline change assessment using geospatial tools: a study on the Ganges deltaic coast of Bangladesh. Earth Sci Inform 13, 299–316 (2020).https://doi.org/10.1007/s12145-019-00423-x

Murat, A., Kale, M.M. & Tekkanat, İ.S. Assessment of the changes in shoreline using digital shoreline analysis system: a case study of Kızılırmak Delta in northern Turkey from 1951 to 2017. Environ Earth Sci 78, 579 (2019).https://doi.org/10.1007/s12665-019-8591-7

Natesan, U., Thulasiraman, N., Deepthi, K., & Kathiravan, K. (2013). Shoreline change analysis of Vedaranyam coast, Tamil Nadu, India. *Environmental Monitoring and Assessment, 185*(6), 5099–5109. https://doi.org/10.1007/s10661-012-2928-y

Pérez-Alberti, A., Pires, A., Freitas, L., & Chaminé, H. (2013). Shoreline change mapping along the coast of Galicia, Spain. *Proceedings of the Institution of Civil Engineers – Maritime Engineering*, *166*(3), 125–144. https://doi.org/10.1680/maen.2012.23

Sestini, G. (1989). Nile Delta: A review of depositional environments and geological history. *Geological Society Special Publication, 41*(1), 99–127. https://doi.org/10.1144/GSL.SP.1989.041.01.09

Stanley, D. J. (1988). Low sediment accumulation rates and erosion on the middle and outer Nile delta shelf off Egypt. *Marine Geology, 84*(1), 111–117. https://doi.org/10.1016/0025-3227(88)90129-6

Stanley, D. J., & Warne, A. G. (1993). Nile Delta: Recent geological evolution and human impact. *Science, 260*(5108), 628–634. https://doi.org/10.1126/science.260.5108.628

Suhura, S., Nithyapriya, B., Revanth-Reddy, L., Philipose, N., Manisha, M., & Dwarakish, G. S. (2018). Coastal land use/land cover and shoreline studies for Dakshina Kannada Coast, Karnataka, India. In V. P. Singh, S. Yadav, & R. N. Yadava (Eds.), *Water Resources Management* (Vol. 78, pp. 269–281). Springer Singapore. https://doi.org/10.1007/978-981-10-5711-3_19

Temitope & Oyedotun. (2014). *Shoreline geometry: DSAS as a tool for historical geometry: DSAS as a tool for historical trend analysis; Temitope D. T. & Oyedotun 1,2 ... The digital shoreline analysis system (DSAS) ...* - [PDF Document]. https://fdocuments.in/document/shoreline-geometry-dsas-as-a-tool-for-historical-geometry-dsas-as-a-tool-for.html

Thieler, E. R., Himmelstoss, E. A., Zichichi, J. L., & Ergul, A. (2017). *The digital shoreline analysis system (DSAS), version 4.0—An ArcGIS extension for calculating shoreline change* (USGS Numbered Series No. 2008–1278; Open-File Report). U.S. Geological Survey. http://pubs.er.usgs.gov/publication/ofr20081278